

Catalysis Science & Technology

Accepted Manuscript



This article can be cited before page numbers have been issued, to do this please use: M. Hoffmann, C. Bizzarri, W. Leitner and T. E. Müller, *Catal. Sci. Technol.*, 2018, DOI: 10.1039/C8CY01691G.



This is an Accepted Manuscript, which has been through the Royal Society of Chemistry peer review process and has been accepted for publication.

Accepted Manuscripts are published online shortly after acceptance, before technical editing, formatting and proof reading. Using this free service, authors can make their results available to the community, in citable form, before we publish the edited article. We will replace this Accepted Manuscript with the edited and formatted Advance Article as soon as it is available.

You can find more information about Accepted Manuscripts in the [author guidelines](#).

Please note that technical editing may introduce minor changes to the text and/or graphics, which may alter content. The journal's standard [Terms & Conditions](#) and the ethical guidelines, outlined in our [author and reviewer resource centre](#), still apply. In no event shall the Royal Society of Chemistry be held responsible for any errors or omissions in this Accepted Manuscript or any consequences arising from the use of any information it contains.



Catal. Sci. Technol.

ARTICLE

Reaction Pathways at the Initial Steps of Trioxane Polymerisation

Matthias Hoffmann,^a Claudia Bizzarri,^{a,b} Walter Leitner^c and Thomas E. Müller^{c,d,*}Received 00th January 20xx,
Accepted 00th January 20xx

DOI: 10.1039/x0xx00000x

www.rsc.org/

Cleavage and (re)formation of oxymethylene moieties are essential steps during the built-up of polyoxymethylene (POM), a technically relevant high-performance polymer. To reveal how the catalyst accomplishes the cleavage of oxymethylene moieties, the kinetics of the ring-opening of trioxane was studied. Thereby insights into the initial phase of the growth of oxymethylene chains were obtained. The chain length of short oligomers was controlled with acetic anhydride as transfer agent. With a high ratio of acetic anhydride to trioxane, the first homologues of the series, trioxymethylene diacetate, dioxymethylene diacetate and monooxymethylene diacetate were obtained in excellent yield. The homologues show distinct features in the NMR and IR spectra that were related to their reactivity during chain propagation. Formation of intermediate hemi-acetal oxonium moieties is suggested to be a key step in the reaction pathway. Such molecular level insight may be a crucial factor for further tailoring production and properties of polyoxymethylene as well as introducing oligomeric oxymethylene diacetates to new application fields.

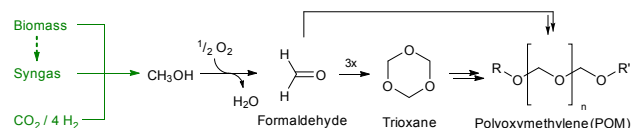
Introduction

Formaldehyde, a base chemical,¹ is produced commercially on a 30 mega ton/a scale² largely by partial oxidation³ (Scheme 1) or dehydrogenation of methanol.⁴ Conventionally, methanol is produced mostly from syngas.^{5,6} Bio-methanol is accessible from renewable raw materials,⁷ e.g. by fermentation of sugar and cellulose based biomass, from syngas obtained by gasification of biomass or by reducing carbon dioxide with hydrogen produced in a renewable manner with electricity from sustainable energy sources.⁸

The option to switch the carbon source to a renewable feedstock renders formaldehyde a stimulating intermediate for the future production of polymers, fuels and chemicals. The trimer of formaldehyde, trioxane, is a likewise interesting intermediate. Simple and energy-efficient processes for the industrial production of trioxane are under development,^{9,10} as the current production process, dating from the 1960s, is energy intensive. Downstream polyoxymethylene (POM) is produced either directly from gaseous formaldehyde or trioxane. More than 800 kt/a POM resins are produced worldwide,¹¹ whereby copolymers represented more than half of the market share.

Gaseous formaldehyde is used in producing homopolymers, such as Delrin-POM, which is acetate-capped.¹² Hydroxy-terminated POM is produced by copolymerising trioxane with small amounts of a comonomer such as ethylene oxide^{11,13} or dioxolane.¹¹ The comonomer introduces oxyethylene moieties into the polymer chain stabilising the chain against depolymerisation.¹⁴

POM finds manifold technical applications as engineering plastics in the automotive, electronics and consumer goods sectors. Its characteristics include outstanding chemical robustness, compatibility with most solvents, low friction and adequate lifetime.¹¹ The highly crystalline POM is readily moulded and extruded. Outstanding mechanical and physical properties are tailored to the requirements of the application by adjusting the fine structure of the polymer scaffold and the type and quantity of comonomers.^{11,12,15,16}



Scheme 1. Formaldehyde, readily accessible from renewable raw materials, is a stimulating C1 polymer building block for the production of polyoxymethylene (POM,^{5,9} R = Initiator, R' = end group) and oligomeric oxymethylene derivatives (this paper) for innovative application fields

^a CAT Catalytic Center, RWTH Aachen University, Worringerweg 2, 52074 Aachen, Germany.

^b Current address: Institute for Organic Chemistry, Karlsruhe Institute for Technology (KIT), Fritz-Haber-Weg 6, 76131 Karlsruhe, Germany

^c Lehrstuhl für Technische Chemie und Petrochemie, ITMC, RWTH Aachen University, Worringerweg 1, 52074 Aachen.

^d Current address: Rheinische Fachhochschule Köln gGmbH, Professur für Verfahrens- und Prozesstechnik, Fachbereich Ingenieurwesen, Schaevenstraße 1a-b, 50676 Köln, Germany; thomas.mueller@rfh-koeln.de

† Footnotes relating to the title and/or authors should appear here.

Electronic Supplementary Information (ESI) available: [experimental details]. See DOI: 10.1039/x0xx00000x

Although POM has been produced commercially for decades, the elementary steps during initiation of the trioxane polymerisation are not yet fully understood.¹⁷⁻²⁰ For solid-acid catalysts, such as AmberlystTM 46, ring-opening of trioxane, followed by the release of molecular formaldehyde, which is consecutively built into the polyoxymethylene chain has been proposed.²¹ As alternative pathway, the direct insertion of trioxane as a trimer into the growing polymer chain has been

ARTICLE

Journal Name

suggested.²⁶ At present, scarce information is available on the initial steps of trioxane polymerisation. Initiation involves several chemical steps, whereby catalyst, a chain-transfer agent, like acetic anhydride, interact with the formaldehyde source. Consequently, this study is aimed at shedding light on how the catalyst impacts the ring-opening of trioxane. Focusing on acetic anhydride as chain-transfer agent, the initial growth of oligomers was followed by *in situ* IR spectroscopy. Kinetic profiles were recorded and the initial steps described with a model involving a direct and an indirect pathway. By determining the corresponding rate constants, the significance of the two pathways was evaluated. Finally, we discuss the plausible mechanism of the trioxane ring-opening reaction in the context of the current findings and suggest to consider the use of oligomeric oxymethylene acetates as fuels with properties similar to dimethylether^{22,23} and other oxygenated fuels.^{24,25}

Results and discussion

Open-chain oxymethylene diacetates, the shortest chain analogues of POM, were obtained by the Brønsted acid-catalysed reaction of trioxane with acetic anhydride (Eq. 1).²⁶ While at low temperatures ($-60\text{ }^{\circ}\text{C}$) trioxymethylene diacetate (TOD, $n = 3$) was obtained as the main product, an equimolar mixture of dioxymethylene diacetate (DOD, $n = 2$) and monooxymethylene diacetate (MOD, $n = 1$) was formed at higher temperatures ($65\text{ }^{\circ}\text{C}$). These oxymethylene diacetates were isolated and further on served as reference compounds.

(1)

In an analogous manner, we targeted at synthesising oligomeric oxymethylene diacetates with $n > 3$ by reacting trioxane with acetic anhydride in a molar ratio of 3:1. The reaction was performed at $0\text{ }^{\circ}\text{C}$ in the presence of catalytic amounts of trifluoromethane sulfonic acid. Unexpectedly, the amount of trioxane built into the diacetates was much lower than anticipated. To obtain insight into the underlying reasons, the course of the reaction was monitored by means of *in situ* IR spectroscopy. Inspection of the IR spectra recorded during the reaction revealed fast conversion of acetic anhydride and trioxane during the initial phase of the reaction (Figure 1). Trioxane conversion slowed down, once acetic anhydride had been fully consumed. This coincided with the formation of a precipitate. After further 10 min, the consumption of trioxane accelerated. With ^1H NMR spectroscopy the chain lengths of the diacetates in the soluble fraction of the product mixture obtained at the end of the reaction (105 min) was determined. The mixture contained MOD (3 mol-%), DOD (13 mol-%), TOD (21 mol-%), tetraoxymethylene diacetate (17 mol-%), pentaoxymethylene diacetate (14 mol-%) and oligomeric

oxymethylene diacetates with higher chain length (32 mol-%, average length of 9.2 units). Overall, the average chain length $n(\text{avg})$ was 5.2, which corresponds to an average molecular weight of 258.8 g/mol. The precipitate that had formed consisted mostly of OH-terminated oligomeric oxymethylene moieties. More detailed analysis of aliquots taken during the course of the reaction revealed that TOD, DOD and MOD were formed only during the initial phase of the reaction as long as acetic anhydride was present. In contrast, oligomeric oxymethylene diacetates were formed over the entire course of reaction.

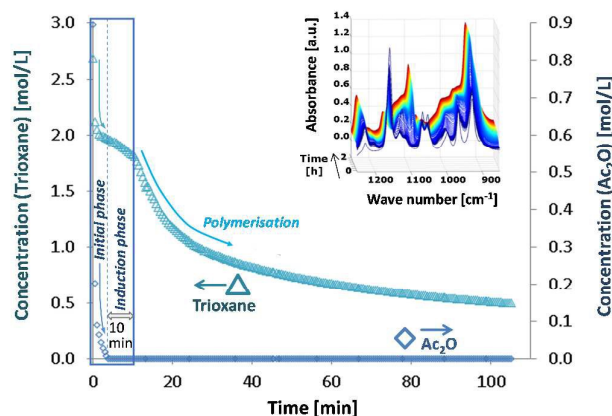


Figure 1. Time-concentration profile of the reaction of trioxane with acetic anhydride in the presence of catalytic amounts of trifluoromethane sulfonic acid ($n(\text{trioxane})/n(\text{Ac}_2\text{O})$ 3/1, dichloromethane, $0\text{ }^{\circ}\text{C}$). Concentrations were determined by convoluting the time-resolved IR spectra (insert, IR spectra taken every 30 s). The concentrations of TOD, DOD, MOD and oligomeric diacetates are omitted for clarity and can be found as supplementary information.

Reaction pathway and kinetics

To obtain more detailed insight into the initial course of the reaction, the $\text{CF}_3\text{SO}_3\text{H}$ -catalysed reaction was repeated with a lower molar ratio of trioxane to acetic anhydride (1:4.5). The profile recorded with *in situ* IR spectroscopy (Figure 2) revealed a fast initial decrease in the intensity of the characteristic bands at 1162 and 1124 cm^{-1} assigned to the $\nu_{\text{as}}(\text{COC})$ ether and ester stretch vibration of trioxane and acetic

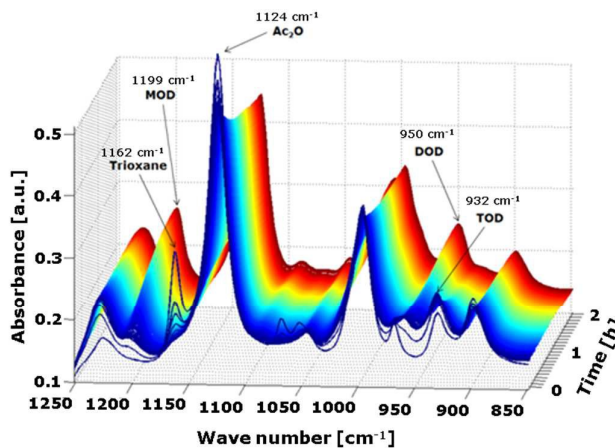


Figure 2. Time-resolved IR profile for the reaction of trioxane with acetic anhydride catalysed by trifluoromethane sulfonic acid ($n(\text{trioxane})/n(\text{Ac}_2\text{O})$ 1/4.5, dichloromethane, 0 °C). The characteristic bands of trioxane, acetic anhydride, TOD, DOD and MOD are highlighted.

anhydride, respectively. In parallel, the intensity of the characteristic band at 932 cm^{-1} , assigned to the $\nu_{\text{sym}}(\text{COC})$ ether stretch vibration of TOD, increased rapidly at the initial time of the reaction. At a later stage the intensity decreased. The intensity of characteristic bands at 950 and 1199 cm^{-1} assigned to the $\nu_{\text{sym}}(\text{COC})$ ether stretch vibration of DOD and the $\nu_{\text{as}}(\text{COC})$ ester stretch vibration of MOD, respectively, increased steadily. Once the trioxane band had vanished (after 190 s), the intensity of the band assigned to acetic anhydride decreased more slowly. The decreasing intensity of the band assigned to TOD was accompanied by the steady increase in the intensity of the bands assigned to DOD and MOD.

To quantify the concentrations, the time-resolved IR spectra were deconvoluted and referenced against calibration spectra of the pure components. The time-concentration profile (Figure 3) revealed that the concentration of trioxane and acetic anhydride decreased quickly during the initial phase of the reaction ($r_{\text{ini}}/c(\text{Cat.})$ -0.482 and -0.531 s^{-1} , respectively). In parallel, the concentration of TOD increased rapidly (0.433 s^{-1}) and that of DOD and MOD more slowly (both 0.049 s^{-1}). After trioxane had been fully converted (after 190 s) the concentration of TOD decreased at a relatively low rate ($r_{\text{max}}/c(\text{Cat.})$ -0.009 s^{-1}). In parallel, the concentrations of DOD and MOD continued to increase. It is noteworthy that the concentrations of DOD and MOD remained equal. This suggests that DOD and MOD are invariably parallel products.

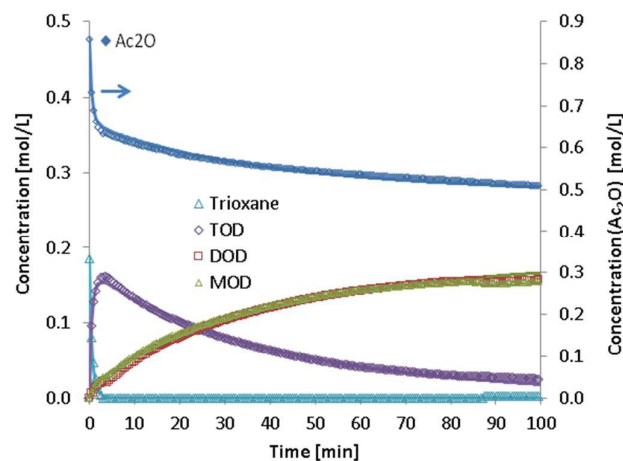
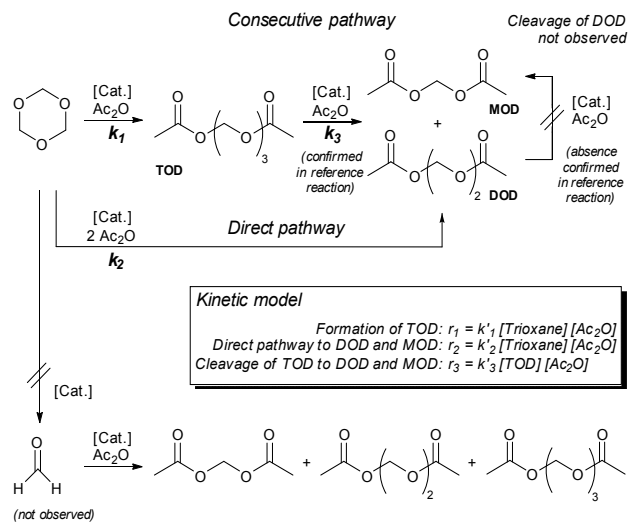


Figure 3. Time-concentration profile of the reaction of trioxane with acetic anhydride catalysed by trifluoromethane sulfonic acid ($n(\text{trioxane})/n(\text{Ac}_2\text{O})$ 1/4.5, CH_2Cl_2 , 0 °C). The continuous lines provide a fit of the data with the model according to Scheme 2.

To obtain further insight into the reaction pathways, the concentration profile was fitted with kinetic models. The profile was described well, when the formation of TOD (r_1) and consecutive cleavage of TOD to DOD and MOD (r_3) as well as the direct cleavage of trioxane to DOD and MOD (r_2) were taken into account (Scheme 2). This kinetic model provided excellent fit with the observed concentrations (Figure 3).

Analysis of the rate constants revealed that the reaction proceeded predominantly *via* the reaction of trioxane with acetic anhydride to TOD ($k_1 = 0.021\text{ (mol/L)}^{-1}\text{ s}^{-1}$). To a smaller extent, DOD and MOD were formed directly from trioxane ($k_2 = 0.002\text{ (mol/L)}^{-1}\text{ s}^{-1}$). The consecutive reaction that converted TOD to DOD and MOD had a much lower rate constant ($k_3 < 0.001\text{ (mol/L)}^{-1}\text{ s}^{-1}$).



Scheme 2. Kinetic model for describing the concentration profiles of the reaction of trioxane with acetic anhydride under the conditions used in this study; $k'_i = k_i [\text{Cat.}]$.

To confirm the consecutive nature of the reaction, TOD was reacted with acetic anhydride (ratio 1:4.9) under the same reaction conditions. The concentration of TOD and acetic anhydride decreased, while DOD and MOD were formed in parallel in equimolar ratio. This proves that TOD is able to react with acetic anhydride to DOD and MOD. To exclude the possibility of an additional consecutive reaction step from DOD to MOD, also DOD was reacted with excess acetic anhydride (ratio 1:4.6) in the presence of catalytic amounts of $\text{CF}_3\text{SO}_3\text{H}$. No conversion was detected. Furthermore, upon closer inspection of the *in-situ* IR spectra, the absence of bands assigned to monomeric formaldehyde was established.

Physicochemical characterisation of oxymethylene diacetates

To understand their reactivity, the isolated oxymethylene diacetates (TOD, DOD and MOD) were fully characterised (see supplementary information).

A downfield shift of the ^1H NMR signal (in CDCl_3) was observed for oxymethylene moieties neighbouring the acetate groups in the sequence TOD (5.30 ppm), DOD (5.32 ppm) and MOD (5.62 ppm). The signal of the internal oxymethylene group in TOD was observed at 4.90 ppm (Table 1). This corresponds to a fairly high electron density for the inner oxymethylene protons of TOD. In comparison, the ^1H NMR signal of the trioxane protons was at 5.15 ppm. Thus, the central oxymethylene moiety in TOD is much less positively polarised than the oxymethylene moieties in trioxane. This implies that likewise to trioxane the inner oxymethylene moiety

ARTICLE

Journal Name

of TOD ought to react readily with electrophiles. In contrast, the oxymethylene moieties neighbouring an acetate groups are positively polarised attenuating the tendency to react with electrophiles.

This is confirmed by close inspection of the IR data. The similar ether stretch vibration (ν_{sym}) of trioxane (930 cm^{-1}) and TOD (932 cm^{-1}) in IR suggest similar reactivity of the oxymethylene moieties. The higher frequency of the ether stretch vibration in DOD (950 cm^{-1}) suggests a lower reactivity. Thus, assuming that the rate determining step involves breakage of the oxymethylene ether bond, the highest reactivity with acetic anhydride ought to be expected for TOD and trioxane. Note that the frequency of the ester stretch vibrations (ν_{sym}) are similar for TOD (1002 cm^{-1}), DOD (1007 cm^{-1}), and MOD (1016 cm^{-1}). The most distinct bands in IR for trioxane (1162 cm^{-1} , $\nu_{\text{as}}(\text{COC})$), acetic anhydride (1124 cm^{-1} , $\nu_{\text{as}}(\text{COC})$), TOD (932 cm^{-1} , $\nu_{\text{sym}}(\text{COC})$), DOD (950 cm^{-1} , $\nu_{\text{sym}}(\text{COC})$) and MOD (1199 cm^{-1} , $\nu_{\text{as}}(\text{COC})$) are separated sufficiently to allow for deconvoluting the IR spectra of reaction mixtures. This makes *in situ* IR spectroscopy an excellent tool for monitoring the course of this reaction.

Table 1 Frequency of the symmetric ether and ester stretch vibrations in oxymethylene diacetates in comparison to trioxane and calculated force constants.

	$\delta(\text{O-CH}_2\text{-O})^a$ [ppm]	ν_{sym} (Ether) [cm^{-1}]	ν_{sym} (Ester) [cm^{-1}]
TOD	5.30/4.90 ^b	932	1002
DOD	5.32	950	1007
MOD	5.62	-	1016
Trioxane	5.15	930	-

^a Chemical shift of the oxymethylene groups in ¹H NMR spectroscopy; ^b outer and inner oxymethylene group, respectively.

Brønsted acid catalysts

To explore the effect of the acid strength, the activity of trifluoromethane sulfonic acid ($\text{CF}_3\text{SO}_3\text{H}$) was compared with other Brønsted acids (Table 2). $\text{CF}_3\text{SO}_3\text{H}$ ($\text{pK}_a = -14$)²⁷ provided an initial rate of trioxane conversion of $r_{\text{ini}}/c(\text{Cat.}) - 0.48\text{ s}^{-1}$ and full conversion within of 200 s. With perchloric acid (HClO_4 , $\text{pK}_a = -10$)^{26,27} there was fast conversion of trioxane, albeit at a lower rate ($r_{\text{ini}}/c(\text{Cat.}) - 0.27\text{ s}^{-1}$; full conversion within of 300 s). In contrast, there was no observable reaction with methane sulfonic acid ($\text{CH}_3\text{SO}_3\text{H}$, $\text{pK}_a = -2.6$)²⁷ *p*-toluene sulfonic acid ($p\text{-CH}_3\text{-C}_6\text{H}_4\text{-SO}_3\text{H}$, $\text{pK}_a = 0.7$)²⁷ and acetic acid (AcOH , $\text{pK}_a = 4.6$)²⁷. This clearly shows that only very strong Brønsted acids catalyse the reaction. Likewise, it was reported that H_2SO_4 ($\text{pK}_a = -3.0$)²⁷ catalyses the reaction.²⁸ The need to employ strong acids is consistent with the low basicity of the substrate trioxane. Apparently, only very strong Brønsted acids can sufficiently activate these substrates.

The higher initial rate with $\text{CF}_3\text{SO}_3\text{H}$ compared to HClO_4 suggests that the activity increases with increasing acidity of the Brønsted acid. The inverse ratio of the rate constant k_1/k_2 and k_1/k_3 for $\text{CF}_3\text{SO}_3\text{H}$ (8.9 and 31, respectively) and HClO_4 (97 and 16, respectively) reveals that the pathway *via* TOD is more pronounced for HClO_4 . Thus, the reaction pathway is

influenced strongly by the nucleophilicity of the anion. The reactivity is reflected also in the ratio of the rate constants k_2/k_3 (3.5 for $\text{CF}_3\text{SO}_3\text{H}$ and 0.16 for HClO_4) suggesting stronger stabilisation of a cationic intermediate by the more polarisable ClO_4^- ion (*vide infra*).

Table 2. Initial rate and product distribution of the reaction of trioxane with acetic anhydride in the presence of Brønsted acid catalysts.

Catalyst		$\text{CF}_3\text{SO}_3\text{H}$	HClO_4
pK_a value		-14	-10
$(r_{\text{ini}})/c(\text{Cat.})$ for trioxane conversion ^a	[s^{-1}]	-0.48	-0.27
k_1/k_2 ^b	[-]	8.9	97
k_1/k_3 ^b	[-]	31	16
k_2/k_3 ^b	[-]	3.5	0.16
Conversion Trioxane ^c	[%]	100	100
Molar ratio TOD / DOD / MOD ^d	[mol-%]	3 / 51 / 46	1 / 51 / 47

^a Initial rate in $\text{mol}_{\text{Trioxane}}(\text{mol}_{\text{Cat.}}\text{ s})^{-1}$; ^b ratio of rate constants determined from the respective time-concentration profile (based on *in situ* IR data). ^c conversion after 2 h; ^d molar ratio in isolated product mixtures.

Lewis acid catalysts

Then the performance of metal triflates as catalysts was explored as their Lewis acidity can be adjusted in a wide range by choosing an appropriate metal +III centre.^{29,30} The influence of the cation radius (hardness)³¹ and the influence of the electronic configuration were studied for the main group metal triflates $\text{Sb}^{\text{III}}(\text{OTf})_3$ (ionic radius $r = 76\text{ pm}$) and $\text{Bi}^{\text{III}}(\text{OTf})_3$ ($r = 103\text{ pm}$) and the transition metal triflates $\text{Sc}^{\text{III}}(\text{OTf})_3$ ($r = 75\text{ pm}$), $\text{Y}^{\text{III}}(\text{OTf})_3$ ($r = 103\text{ pm}$), and $\text{La}^{\text{III}}(\text{OTf})_3$ ($r = 103\text{ pm}$). With $\text{Sb}^{\text{III}}(\text{OTf})_3$ trioxane was converted fast at an initial rate ($r_{\text{ini}}/c(\text{Cat.})$) of -0.61 s^{-1} , and full conversion was achieved within 100 s. Similarly, with $\text{Bi}^{\text{III}}(\text{OTf})_3$ trioxane was converted fast (full conversion within of 300 s) at an initial rate ($r_{\text{ini}}/c(\text{Cat.})$) of -0.35 s^{-1} . In contrast, with $\text{Sc}^{\text{III}}(\text{OTf})_3$ trioxane was converted more slowly at an initial rate of -0.14 s^{-1} and full conversion was obtained within 3000 s. With $\text{Y}^{\text{III}}(\text{OTf})_3$ trioxane was converted very slowly ($r_{\text{ini}}/c(\text{Cat.}) = -0.0012\text{ s}^{-1}$) and conversion was only 37 % after 2 h of reaction time. With $\text{La}^{\text{III}}(\text{OTf})_3$ there was no detectable reaction within of 2 h. Thus, a higher activity was found for main group elements compared to their early transition metal Lewis acid counterparts with similar radius. Thus, the main group Lewis acids are more active compared to the closed-shell early transition metals, most likely due to their open shell configuration.

The activity of the Lewis acid catalysts increased with the decreasing radius of the metal cation within the chosen main group and transition metal series. For instance, $\text{Sb}^{\text{III}}(\text{OTf})_3$ gave a 1.7-fold higher rate compared to $\text{Bi}^{\text{III}}(\text{OTf})_3$. Similarly, $\text{Sc}^{\text{III}}(\text{OTf})_3$ gave a 120 times higher rate compared to $\text{Y}^{\text{III}}(\text{OTf})_3$. Hence, small cations, corresponding to hard Lewis acids, resulted in higher rates. The formation of DOD and MOD was significantly less pronounced for $\text{Sc}^{\text{III}}(\text{OTf})_3$, or did not occur at all for $\text{Y}^{\text{III}}(\text{OTf})_3$, compared to the main group counterparts.

This is also reflected by the ratios of the determined rate constants (Table 3). The ratio of the rate constant k_1/k_2 and k_1/k_3 were similar for $\text{Sb}^{\text{III}}(\text{OTf})_3$ (3.9 and 13, respectively), $\text{Bi}^{\text{III}}(\text{OTf})_3$ (6.3 and 32.7, respectively). In contrast, $\text{Sc}^{\text{III}}(\text{OTf})_3$ (22 and 1400, respectively) and $\text{Y}^{\text{III}}(\text{OTf})_3$ (no secondary reactions) were highly selective to TOD formation. Moreover,

the ratios of the rate constants k_2/k_3 of $\text{Sb}^{\text{III}}(\text{OTf})_3$ (3.5) and $\text{Bi}^{\text{III}}(\text{OTf})_3$ (5.2) compared to $\text{Sc}^{\text{III}}(\text{OTf})_3$ (67.2) underline a different selectivity of main group and early transition metal triflates. In a reference experiment, trioxane was reacted in dichloromethane solution in the presence of catalytic amounts of $\text{Sc}^{\text{III}}(\text{OTf})_3$ (1 mol-%) at room temperature. Even after three days no reaction was observed. This shows that the presence of acetic anhydride is required for $\text{Sc}^{\text{III}}(\text{OTf})_3$ to be able to convert trioxane.

Table 3. Initial rate and product distribution of the reaction of trioxane with acetic anhydride in the presence of Lewis acid catalysts.

Catalyst		$\text{Sb}^{\text{III}}(\text{OTf})_3$	$\text{Bi}^{\text{III}}(\text{OTf})_3$	$\text{Sc}^{\text{III}}(\text{OTf})_3$	$\text{Y}^{\text{III}}(\text{OTf})_3$
r	[$\mu\text{mol L}^{-1} \text{s}^{-1}$]	76	103	75	103
$r_{\text{ini}}/c(\text{Cat.})$ for trioxane conversion ^a	[s^{-1}]	-0.61	-0.35	-0.14	-0.0012
k_1/k_2 ^b	[-]	3.9	6.3	22	-
k_1/k_3 ^b	[-]	13	32.7	1.4×10^3	-
k_2/k_3 ^b	[-]	3.5	5.2	67	-
Conv. of trioxane ^c	[%]	100	100	100	37
Molar ratio TOD/DOD/MOD ^d	[mol-%]	15/44/41	15/45/40	71/15/14	37/0/0

^a Initial rate in $\text{mol}_{\text{trioxane}}(\text{mol}_{\text{cat}} \text{s})^{-1}$; ^b ratio of rate constants determined from the respective time-concentration profile (based on *in situ* IR data). ^c conversion after 2 h; ^d molar ratio in isolated product mixtures.

As with Brønsted acid catalysts, the extent of consecutive reactions was explored for Lewis acid catalysts. Thus, TOD was reacted with an excess of acetic anhydride in the presence of either $\text{Bi}^{\text{III}}(\text{OTf})_3$ or $\text{Sc}^{\text{III}}(\text{OTf})_3$. As with Brønsted acid catalysts, DOD and MOD formed in equimolar ratios. The use of the harder Lewis acid $\text{Bi}^{\text{III}}(\text{OTf})_3$ resulted in higher conversion compared to $\text{Sc}^{\text{III}}(\text{OTf})_3$, in agreement with the above-described trends in catalyst activity.

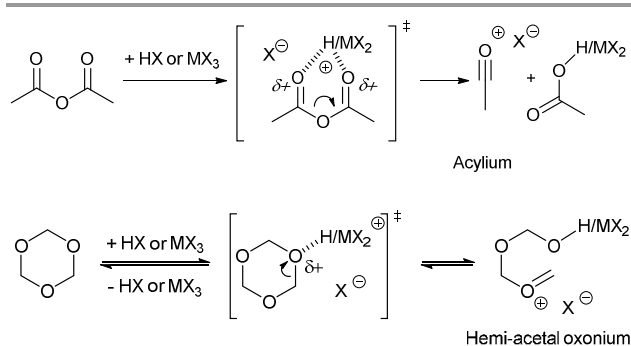
Role of the catalyst

Analysis of the potential role of the catalyst in the reaction of trioxane with acetic anhydride revealed two modes of how the substrates can be activated (Scheme 3). The carboxyl oxygen atom of acetic anhydride is susceptible to protonation by a Brønsted acid or coordination by a Lewis acid. This activates acetic anhydride to be cleaved into an acylium cation and acetic acid or a coordinated acetate ion, respectively (Scheme 3, top). Likewise, the oxygen atom of trioxane is susceptible to protonation by a strong Brønsted acid or coordination to a Lewis acid, whereby ring-opening and formation of a hemiacetal oxonium ion may be triggered (Scheme 3, bottom).

Activation of acetic anhydride seems more likely than activation of trioxane. This claim is supported by the reduced rate of trioxane conversion, which was observed once all acetic anhydride had been consumed. Considering the initial rate of trioxane conversion, the catalyst activity decreased in the sequence $\text{CF}_3\text{SO}_3\text{H} > \text{Bi}^{\text{III}}(\text{OTf})_3 > \text{Sc}^{\text{III}}(\text{OTf})_3$. A similar trend in catalyst activity had been reported for the related Friedel Crafts acylation of toluene with benzoic anhydride.³² Activation of the anhydride to the corresponding acylium ion as key intermediate had been proposed.

In the next step (Scheme 4), the acylium cation is proposed to react with trioxane resulting in the cationic acylium trioxane

intermediate **11**. Opening of the trioxane ring provides the hemiacetal oxonium intermediate **12**. Reaction with acetic anhydride or acetic acid provides TOD. There are two pathways for formation of DOD and MOD. (i) In the direct pathway to DOD and MOD the hemiacetal oxonium intermediate **12** reacts with acetic anhydride, whereby a single oxymethylene unit is transferred in a concerted manner to form MOD. Thereby, the hemiacetal oxonium intermediate is shortened by one oxymethylene unit to intermediate **14**. Reaction with acetic anhydride or acetic acid provides DOD. (ii) In the consecutive pathway to DOD and MOD an acylium ion reacts with TOD to form intermediate **15**. Later is cleaved to MOD and to intermediate **14**. Reaction with acetic anhydride or acetic acid provides DOD. Both pathways provide an equimolar ratio of DOD and MOD.



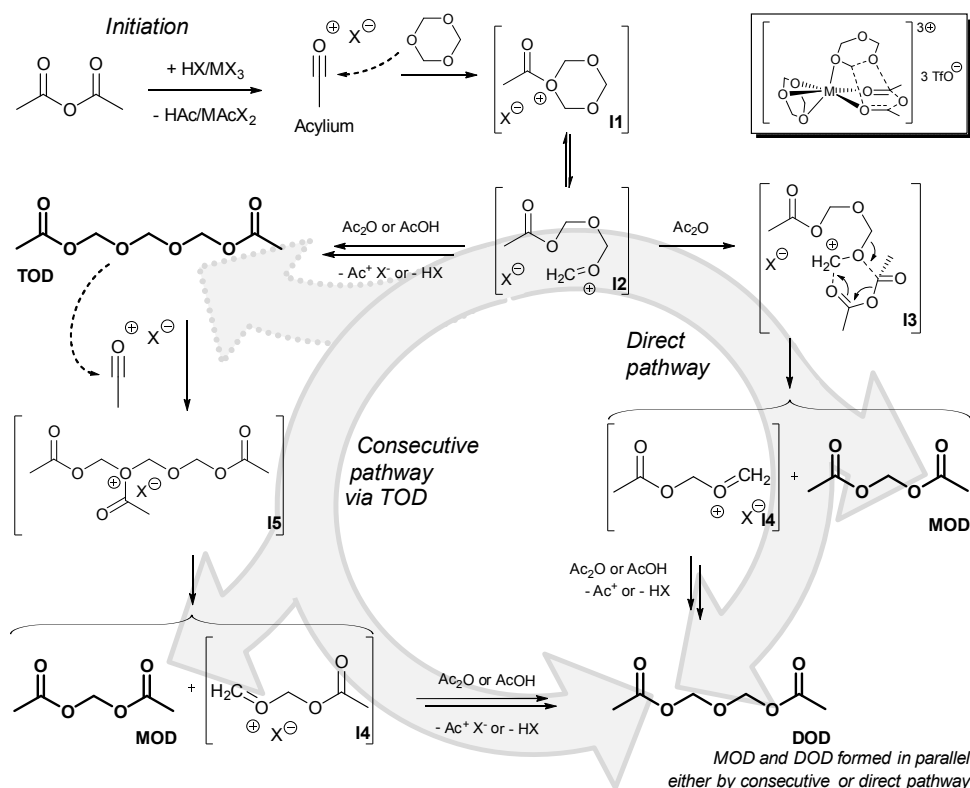
Scheme 3 Potential activation modes for acetic anhydride (top) and trioxane (bottom) by Brønsted acid (HX) and Lewis acid (MX_3) catalysts leading to formation of an acylium cation or hemiacetal oxonium, respectively.

Accordingly, trioxane reacts either with one acetic anhydride molecule to TOD or with two molecules of acetic anhydride to DOD and MOD. A relationship between the anion X^- of the catalyst and the selectivity becomes obvious upon comparing the ratio k_2/k_3 for $\text{CF}_3\text{SO}_3\text{H}$ (3.48) and HClO_4 (0.16). Both pathways are feasible in the presence of $\text{CF}_3\text{SO}_3\text{H}$, while the consecutive pathway is much more strongly pronounced in the presence of HClO_4 . The CF_3SO_3^- anion is a weaker nucleophile compared to ClO_4^- , reflected in the higher acidity of the corresponding trifluoromethane sulfonic acid. Most likely, the better separation of the ion pair **12** in case of $\text{CF}_3\text{SO}_3\text{H}$ facilitates the concerted transfer of the single oxymethylene unit *via* **13**. In contrast, in the presence of the stronger nucleophile ClO_4^- intermediate **12** is more stabilised. Consequently, the consecutive pathway is favoured.

Noteworthy, in the presence of excess acetic anhydride, TOD was cleaved in the presence of catalyst. In contrast, DOD was stable under our reaction conditions. Closer inspection of the corresponding NMR data of TOD reveals a significant high-field shift signal of the inner oxymethylene groups ($\delta_{\text{H}} = 4.90$ ppm, $\delta_{\text{C}} = 92.3$ ppm) compared to the corresponding oxymethylene groups that have neighbouring acetate units ($\delta_{\text{H}} = 5.30$ ppm, $\delta_{\text{C}} = 85.4$ ppm). The oxymethylene units of DOD

Catal. Sci. Technol.

ARTICLE



Scheme 4 Proposed mechanism of ring-opening and cleavage of trioxane in the presence of acetic anhydride as chain transfer agent and Brønsted acid or late transition metal triflate catalyst ($M = \text{Sb}, \text{Bi}$) and transition state of the concerted pathway with early transition metal triflate catalysts ($M = \text{Sc}, \text{Y}$, insert).

($\delta_{\text{H}} = 5.32 \text{ ppm}$, $\delta_{\text{C}} = 86.7 \text{ ppm}$) are very similar to the acetate neighbored oxymethylene units of TOD. Thus, the high electron density at the inner oxymethylene groups that is reflected in the high-field shift facilitates the reaction of the acylium ion with TOD to form intermediate **15**. Apparently, for DOD the electron density at the oxymethylene unit is insufficient to allow for reaction with the acylium ion.

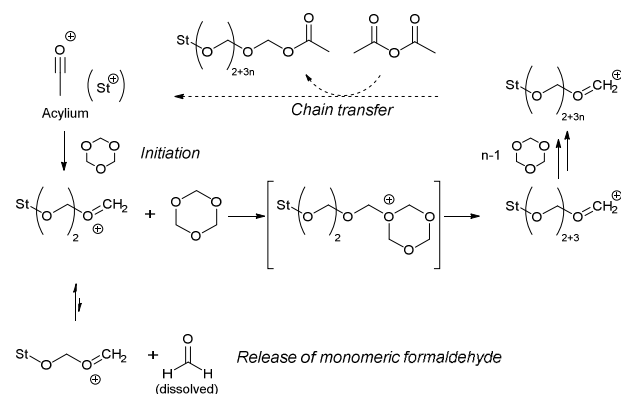
In contrast, the $\text{Sc}^{\text{III}}(\text{OTf})_3$ -catalysed reaction may follow an alternative mechanism, as considerably higher ratios of k_1/k_2 (21.5) and k_1/k_3 (1441) were determined even though, a similar ratio was expected due to the triflate ligands. Also, the reaction was second-order with respect to trioxane. We propose that a second trioxane molecule is required as ligand at the scandium metal centre to achieve the right electronic density to catalyse the reaction between acetic anhydride and an incoming trioxane molecule. We suggest the reaction to proceed predominantly *via* an inner-sphere concerted transition state (Scheme 4, insert). The much lower overall rate can be explained in two

ways: First, the concerted transition state requires a particular orientation of the molecules. The low probability of adopting the appropriate orientation lowers the overall rate of reaction. Second, the effective concentration of acylium cations may be lower, since in the concerted first reaction step the substrates compete for $\text{Sc}^{\text{III}}(\text{OTf})_3$ as the reaction partner. Interestingly, $\text{Y}^{\text{III}}(\text{OTf})_3$ catalysed only the formation of TOD albeit at a low rate that is reflected in the low conversion of trioxane of 37%. The formation of DOD and MOD was not observed. Being a soft Lewis acid, the yttrium catalysed reaction most likely proceeds only *via* the concerted transition state.

Mechanism of the cationic oligomerisation of trioxane

With respect to the formation of oligomeric oxymethylene diacetates with $n > 3$ we propose that a similar mechanism is adopted. The low reaction temperature well below the ceiling temperature³³ does not favour the formation of monomeric formaldehyde. We propose that chain growth occurs in a

similar manner as described above by nucleophilic attack of a hemi-acetal oxonium intermediate on trioxane (Scheme 6). Acetic anhydride functions as chain-transfer agent, and an acylium ion is released, when a growing chain is terminated. Such chain-transfer is known for many polar compounds, such as water, methanol, dimethoxymethane, esters and acid anhydrides as well as some olefins and aromatics.³⁴⁻³⁸ Thereby an end group is introduced, while the released cationic component initiates a new growing chain. Compared to the initiation reaction with acetic anhydride re-initiation of an oxymethylene diacetate moiety is less favoured. Consequently, chain growth commences once acetic anhydride had been fully consumed. This readily explains the preferential formation of oligomeric oxymethylene diacetates. Later are formed by several consecutive chain growth steps before the terminal hemi-acetal oxonium reacts with another nucleophile. The precipitate is undoubtedly formed, when the chain growth reaction dominates.



Scheme 5. Mechanism proposed for chain growth during the ring-opening oligomerisation of trioxane (St = initiator).³⁹ The low reaction temperature does not favour the formation of monomeric formaldehyde.^{33,39}

Considering the mass balance, the extent of termination reactions must be very low. In case of Brønsted acid catalysts, reaction of the hemi-acetal oxonium intermediate with acetic acid formed during initiation regenerates the catalyst. Termination occurs in the presence of excess protic species as it is known for instance with alcohols.^{40,41} Also occlusion^{41,42} of the chain end in the bulk of the precipitating crystalline polymer may terminate the cationic oligomerisation of trioxane. This may explain the above-mentioned gradual decrease in the rate of trioxane consumption. Work-up involved quenching the reaction mixture with a saturated aqueous solution of sodium carbonate. Alternatively, chain growth can be terminated by addition of basic compounds such as sodium alkoxides.⁴³ Another termination method employs alkyl and aryl phosphines, which results in trapping of growing chains as quaternary phosphonium salts.⁴⁴

Experimental

Synthesis of oxymethylene diacetates²⁶

A mixture of acetic anhydride (94 mL, 1 mol) and perchloric acid (70 %, 0.2 mL, 0.0023 mol) was cooled to -60 °C. Trioxane (19.831 g, 0.22 mol) was added over 10 minutes and the reaction mixture stirred for one hour. Then the reaction mixture was poured into a saturated aqueous solution of sodium carbonate (200 mL). The mixture was extracted four times with diethyl ether (50 mL). The combined organic phases, containing a high percentage of TOD (Table 4), were dried over Na₂SO₄, the volatiles removed under partial vacuum and TOD isolated by distillation of the crude product mixture at reduced pressure (1 mbar).

Table 4. Composition of the crude reaction mixtures

Entry ^a	Temp. [°C]	TOD [mol-%]	DOD [mol-%]	MOD [mol-%]
1	-60 °C	78	13	9
2	65 °C	0	39	61

^a The yields of TOD, DOD and MOD together are 78 wt-% and 80 wt-% for entries 1 and 2, respectively.

A mixture of acetic anhydride (47 mL, 0.5 mol) and perchloric acid (70 %, 0.1 mL, 0.0012 mol) was heated to 63 °C. Trioxane (9.926 g, 0.11 mol) was added over 10 minutes and the reaction mixture stirred for another 10 minutes. Then, the reaction mixture was poured into a saturated aqueous solution of sodium carbonate (200 mL). The mixture was extracted four times with diethyl ether (50 mL). The combined organic phases, containing a high percentage of DOD and MOD (Table 4), were dried over Na₂SO₄. The volatiles were removed in a partial vacuum and DOD and MOD isolated by fractionated distillation of the crude mixture at reduced pressure (1 mbar).

Trioxymethylene diacetate (TOD)

δ_{H} (400 MHz, CDCl₃) = 1.99 (s, 6 H, C(O)CH₃), 5.30 (s, 4 H, AcOCH₂OCH₂OCH₂OAc), 4.90 (s, 4 H, OCH₂OCH₂OCH₂O).

δ_{C} (100 MHz, CDCl₃) = 20.7 (H₃C(O)-), 85.4 (AcOCH₂OCH₂OCH₂OAc), 92.3 (AcOCH₂OCH₂OCH₂OAc) 170.1 (H₃C(O)-).

$\nu_{\text{max}}/\text{cm}^{-1}$: 2983 (w, CH₃), 2921 (w, CH₂), 1742 (s, C=O), 1465 (w), 1428 (w), 1368 (w, CH₃), 1222 (s, ν_{as} ester), 1204 (w, ν_{as} ester), 1165 (w, ν_{as} ether), 1127 (s, ν_{as} ether), 1049 (w), 999 (s, ν_{sym} ester), 955 (w, ν_{sym} ester), 930 (vs, ν_{sym} ether), 833 (w), 607 (w), 534 (w).

m/z (CI): 326.3 (<1 %), 325.3 (4), 297.3 (3), 296.3 (12), 295.3 (100, M⁺ + Ac₂O + H), 294.7 (2, M⁺ + Ac₂O), 267.3 (1), 266.2 (6), 265.3 (63, M⁺ + Ac₂O + H - CH₂=O), 205.3 (<1, 2 × Ac₂O + 1), 103.2 (5).

Elemental analysis

Found: C, 43.6; H, 6.45. Calc. for C₇H₁₂O₆, 43.75; H, 6.45 wt.-%

Dioxymethylene diacetate (DOD)

δ_{H} (400 MHz, CDCl₃) = 2.00 (s, 6 H, C(O)CH₃), 5.32 (s, 4 H, OCH₂OCH₂O).

δ_{C} (100 MHz, CDCl₃) = 20.7 (H₃C(O)-), 86.7 (AcOCH₂OCH₂OAc), 170.0 (H₃C(O)-).

$\nu_{\text{max}}/\text{cm}^{-1}$ = 2983 (w, CH₃), 2927 (w, CH₂), 1744 (s, C=O), 1461 (w), 1426 (w), 1368 (w, CH₃), 1219 (s, ν_{as} ester), 1187 (w, ν_{as} ester), 1142 (s, ν_{as} ether), 1087 (s, ν_{as} ether), 1029 (w, ν_{sym} ester), 1004 (s, ν_{sym} ester), 937 (vs, ν_{sym} ether), 832 (w), 606 (w), 550 (w).

m/z (EI) = 267.2 (<1 %), 266.1 (2), 265.1 (20, M⁺ + Ac₂O + H), 205.1 (4, 2 × Ac₂O + 1), 146.1 (<1), 145.1 (8), 104.1 (5), 103.2 (100, Ac₂O + H), 102.2 (<1), 73.2 (10).

Elemental analysis

Found: C, 44.25; H, 6.1. Calc. for C₆H₁₀O₅, 44.45; H, 6.2 wt.-%

Monooxymethylene diacetate (MOD)

δ_{H} (400 MHz, CDCl_3) = 2.00 (s, 6 H, $\text{C}(\text{O})\text{CH}_3$), 5.62 (s, 2 H, AcOCH_2OAc).

δ_{C} (100 MHz, CDCl_3) = 20.5 ($\text{H}_3\text{CC}(\text{O})-$), 79.0 (AcOCH_2OAc), 169.5 ($\text{H}_3\text{CC}(\text{O})-$).

$\nu_{\text{max}}/\text{cm}^{-1}$ = 2994 (w, CH_3), 2945 (w, CH_2), 1757 (s, C=O), 1453 (w), 1431 (w), 1368 (w, CH_3), 1239 (w, ν_{as} ester), 1189 (vs, ν_{as} ester), 1084 (w), 1065 (w), 1047 (w), 1004 (vs, ν_{sym} ester), 977 (s, ν_{sym} ether), 820 (w), 666 (w), 605 (w), 518 (w), 456 (w).

m/z (ESI) = 167.3 (12 %), 157.2 (22), 155.1 (11), 150.0 (63.2), 143.1 (16), 133.9 (4, $\text{M}^+ + \text{H}$), 132.9 (100, M^+), 103.1 (26, $\text{Ac}_2\text{O} + \text{H}$), 102.2 (85, Ac_2O), 69.1 (48).

Elemental analysis

Found: C, 45.2; H, 6.25. Calc. for $\text{C}_3\text{H}_8\text{O}_4$ C, 45.5; H, 6.1 wt.-%

General procedure of kinetic experiments

A background measurement with dichloromethane (30 mL) was performed at 0 °C with an *in-situ* IR probe. Trioxane and acetic anhydride were added, and the *in-situ* IR measurement was started. The catalyst (Table 5, Table 6, Table 7, and Table 8) was added to the reaction mixture at 0 °C, which was then stirred for 2 h at 0 °C. The reaction mixture was poured into a saturated aqueous solution of sodium carbonate (50 mL). The organic layer was separated and washed with water (50 mL) and, after another separation, was washed with brine (50 mL). The organic layer was then dried with sodium sulphate and the solvent removed *in vacuo*.

Table 5. Quantities employed in the Brønsted acid catalysed reaction of trioxane with acetic anhydride and selected experimental data.

Catalyst		$\text{CF}_3\text{SO}_3\text{H}$	HClO_4	$\text{CH}_3\text{SO}_3\text{H}$
Trioxane	[mmol]	6.01	5.96	6.06
Acetic anhydride	[mmol]	26.9	26.4	25.66
Catalyst	[mmol]	0.227	0.255	0.274
Conv. Trioxane ^a	[%]	100	100	No reaction
Ratio TOD/DOD/MOD ^a	[mol-%]	3/51/46	1/51/47	-
Yield ^b	[g]	2.70	2.55	0.637

^a Molar ratio in isolated product mixtures and conversion of trioxane. ^b Yields are reported for product mixture isolated after aqueous work up.

Table 6. Quantities employed in the Lewis acid catalysed reaction of trioxane with acetic anhydride and selected experimental data.

Catalyst		$\text{Sb}^{\text{III}}\text{OTf}_3$	$\text{Bi}^{\text{III}}\text{OTf}_3$	$\text{Sc}^{\text{III}}\text{OTf}_3$	$\text{Y}^{\text{III}}\text{OTf}_3$
Trioxane	[mmol]	5.89	6.03	6.08	6.08
Acetic anhydride	[mmol]	25.3	26.5	24.9	26.4
Catalyst	[mmol]	0.260	0.259	0.483	0.257
Conv. Trioxane ^a	[%]	100	100	100	37
Ratio TOD/DOD/MOD ^a	[mol-%]	15/44/41	15/45/40	71/15/14	37/0/0
Yield ^b	[g]	2.3	2.32	2.75	3.28

^a Molar ratios in isolated product mixtures and conversions relative to the amount of trioxane employed. ^b Yields are reported for the amount of product mixture isolated after aqueous work up.

Table 7. Quantities employed in the Lewis acid catalysed reaction of trioxane with acetic anhydride in comparison to the corresponding Brønsted acid catalysed reaction with $\text{CF}_3\text{SO}_3\text{H}$ and selected experimental data.

Catalyst		$\text{CF}_3\text{SO}_3\text{H}$	$\text{Bi}^{\text{III}}\text{OTf}_3$	$\text{Sc}^{\text{III}}\text{OTf}_3$
Trioxane	[mmol]	5.00	5.00	6.44
Acetic anhydride	[mmol]	24.4	24.5	26.3
Catalyst	[mmol]	0.227	0.243	0.221
Conv. Trioxane ^a	[%]	73	73	11
Ratio TOD/DOD/MOD ^a	[mol-%]	16/44/40	17/46/36	82/10/8
Yield ^b	[g]	1.84	1.79	2.04

^a Molar ratio in isolated product mixtures and conversion of TOD. ^b Yields are reported for product mixture isolated after aqueous work up.

Table 8. Quantities employed in the Brønsted acid catalysed reaction of DOD with acetic anhydride, Lewis acid catalysed reaction of trioxane with acetic anhydride and selected experimental data.

Catalyst		$\text{CF}_3\text{SO}_3\text{H}^{\text{a}}$	$\text{Sc}^{\text{III}}\text{OTf}_3^{\text{b}}$
DOD	[mmol]	5.75	-
Acetic anhydride	[mmol]	26.3	-
Trioxane	[mmol]	-	11.5
Catalyst	[mmol]	0.227	0.110
Conversion	[%]	No reaction	No reaction

^a 30 mL DCM, 0 °C, 2h ^b 10 mL DCM, 25 °C, 3 days

Determination of time-concentration profiles

Time-resolved IR spectra were deconvoluted using PEAXACT software,⁴⁵ whereby the IR bands were described by Lorentz functions accounting for changes in the position of the peak with concentration. Initial rates were calculated by fitting the time-concentration profile with a polynomial function and subsequent extrapolation of the first derivative to zero time.

Conclusions

To obtain insight in how the catalyst impacts the initial phase of the growth of the oxymethylene polymer chain, the ring-opening reaction of trioxane with acetic anhydride was studied in detail. The first homologues of the series, trioxymethylene diacetate (TOD), dioxymethylene diacetate (DOD), and monooxymethylene diacetate (MOD), were isolated and fully characterised. Noteworthy is the upfield shift of the signal of the inner oxymethylene protons in TOD in ¹H NMR spectroscopy. Accordingly, TOD showed high reactivity comparable to that of trioxane. Kinetic profiles recorded for the reaction of trioxane with acetic anhydride in the presence of a Brønsted or Lewis acidic catalyst revealed TOD to be a key intermediate. TOD was found to be a primary reaction product formed by the direct incorporation of trioxane into acetic anhydride. To a lower extent, also MOD and DOD were formed directly by reaction of one trioxane with two acetic anhydride molecules. This direct formation was ascribed to the cleavage of a hemi-acetal oxonium intermediate (**12**) with acetic anhydride. Noteworthy DOD was no further cleaved with acetic anhydride under our reaction conditions to MOD moieties. In the contrary, TOD was cleaved readily with acetic anhydride to equimolar amounts of MOD and DOD. Thus, two pathways were present accounting for the formation of DOD and MOD.

The extent to which the two reaction pathways are followed depends critically on the choice of the catalyst. By fitting a kinetic model of the reaction sequence to the recorded reaction profiles, the corresponding rate constants for the individual reaction steps were determined for different Brønsted acid and Lewis acid catalysts. For Brønsted acid catalysts, the rate of trioxane conversion increased with increasing acidity of the catalyst. Noteworthy, the reaction pathway with Brønsted acid catalysts showed a strong influence on the corresponding anion. Trifluoromethane sulfonic acid ($pK_a = 14$) catalysed predominantly the direct pathway for DOD and MOD formation. In contrast, perchloric acid ($pK_a = -10$) catalysed mostly the formation of DOD and MOD *via* the consecutive pathway. We believe that the higher nucleophilic character of the perchlorate stabilises the cationic intermediates by more pronounced cation/anion interactions.

For Lewis acid catalysts, the activity was found to increase with the hardness of the cation. Also the electron configuration had a strong influence on the activity of the catalyst. The main group Lewis acids $Sb^{III}(OTf)_3$ and $Bi^{III}(OTf)_3$ with their open shell configuration provided much higher activity compared to the transition metal Lewis acids $Sc^{III}(OTf)_3$ and $Y^{III}(OTf)_3$. Also the reaction order with respect to trioxane differed for Brønsted and main group Lewis acid catalysts (first order) and transition metal Lewis acid catalysts (second order). While relative rate constants were similar for Brønsted and main group Lewis acid catalysts, transition metal Lewis acid catalysts had very different rate constants. Accordingly, we propose two alternative reaction mechanisms for the ring-opening reaction between trioxane and acetic anhydride. Brønsted acid and main group Lewis acid catalysts most likely follow a cationic reaction mechanism, while the transition metal Lewis acids follow a neutral concerted reaction mechanism. The formation of hemi-acetal oxonium intermediates with Brønsted acid and main group Lewis acid catalysts likewise accounts for the cationic oligomerisation in the presence of excess trioxane. Acetic anhydride thereby functions as chain-transfer agent, whereby a new acylium ion is released, when a growing chain is terminated.

In summary, trifluoromethane sulfonic acid and bismuth (III) triflate were identified as promising catalysts for the ring-opening oligomerisation of trioxane and cyclic anhydrides. Oxymethylene diacetates with low molecular weight and similar products obtained by ring-opening of trioxane with other chain-transfer agents, like methanol or dimethoxymethane (DMME), have an interesting property profile. Application fields of these highly oxygen containing oxymethylene derivatives include the use as sustainable fuels.

Conflicts of interest

There are no conflicts to declare.

Acknowledgements

We acknowledge scientific discussions with Dr. Henning Vogt and Dr. Burkhard Köhler. We thank Volker Marker, Alexandra Keldenich and Mario Krautschick for experimental support. Dirk Engels (S-PACT) is acknowledged for support in deconvoluting the IR spectra.

Notes and references

- G. Reuss, W. Disteldorf, A. O. Gamer, A. Hilt, Ullmann's Encyclopaedia of Industrial Chemistry, 2012, Vol. 15, Wiley-VCH, Weinheim, p. 735-768.
- L. E. Heim, H. Konnerth and M. H. G. Prechtl, *Green Chemistry*, 2017, **19**, 2347.
- M. D. Thomas, *Journal of the American Chemical Society*, 1920, **42**, 873.
- S. Su, P. Zaza and A. Renken, *Chemical Engineering Technology*, 1994, **17**, 34.
- S. Wesselbaum, T. Vom Stein, J. Klankermayer, W. Leitner, *Angewandte Chemie International Edition*, 2012, **51**, 7499.
- J. Klankermayer, S. Wesselbaum, K. Beydoun and W. Leitner, *Angewandte Chemie International Edition*, 2016, **55**, 7296.
- A. S. Suntana, K. A. Vogt, E. C. Turnblom, R. Upadhye, *Applied Energy*, 2009, **86**, S215.
- J. Artz, T. E. Müller, K. Thenert, J. Kleinekorte, R. Meys, A. Sternberg, A. Bardow and W. Leitner, *Chemical Reviews*, 2018, **118**, 434.
- T. Grützner, H. Hasse, N. Lang, M. Siegert and E. Ströfer, *Chemical Engineering*, 2007, **62**, 5613.
- M. Siegert, N. Lang, E. Ströfer, A. Strammer, T. Friese, H. Hasse, Deutsches Patent, DE10361516.
- S. Lüftl, P.M. Visakh, S. Chandran, *Polyoxymethylene Handbook*, Wiley VCH, 1st Edition, 2014.
- a) N. R. MacDonald, US Pat., 2 768 994, 1956; b) C. E. Schweitzer, R. N. MacDonald and J. O. Punderson, *Journal of Applied Polymer Science*, 1959, **2**, 158.
- J. Majer, O. Hainova, *Kolloid-Zeitschrift*, 1965, **1**, 23.
- C. Bizzarri, H. Vogt, G. Baráth, W. Leitner, T. E. Müller, *Green Chemistry* 2016, **18**, 5160-5168.
- C. F. Hammer, T. A. Koch and J. F. Whitney, *Journal of Applied Polymer Science*, 1959, **1**, 169.
- W. H. Linton and H. H. Goodman, *Journal of Applied Polymer Science*, 1959, **1**, 179.
- V. Jaacks and W. Kern, *Die Makromolekulare Chemie*, 1963, **62**, 1.
- Y.-T. Shieh, M.-J. Yeh and S.-A. Chen, *Journal of Polymer Science, A: Polymer Chemistry*, 1999, **37**, 4198.
- Y.-T. Shieh and S.-A. Chen, *Journal of Polymer Science, A: Polymer Chemistry*, 1999, **37**, 483.
- J. Masamoto, K. Matsuzaki, T. Iwaisako, K. Yoshida, K. Kagawa and H. Nagahara, *Journal of Applied Polymer Science*, 1993, **50**, 1317.
- J. Burger, E. Ströfer and H. Hasse, *Industrial & Engineering Chemistry Research*, 2012, **51**, 12751.
- E. Catizzone, G. Bonura, M. Migliori, F. Frusteri, G. Giordano, *Molecules* 2011, **23**(1), 31/1-31/28.
- S. Roy, A. Cherevotan, S. C. Peter, *ACS Energy Letters* 2018, **3**(8), 1938-1966.
- S. E. Iannuzzi, C. Barro, K. Boulouchos, J. Burger, Jakob, *Fuel* 2016, **167**, 49-59.

- ²⁵ E. Ranzi, A. Frassoldati, R. Grana, A. Cuoci, T. Faravelli, A. P. Kelley, C. K. Law, *Progress in Energy and Combustion Science* 2011, **38**(4), 468-501.
- ²⁶ J. Tomiška and E. Spousta, *Angewandte Chemie*, 1962, **74**, 248.
- ²⁷ Evans pK_a table: http://evans.rc.fas.harvard.edu/pdf/evans_pKa_table.pdf
- ²⁸ W. D. King and D. J. Stanonis, *Journal of Applied Polymer Science*, 1974, **18**, 547.
- ²⁹ S. Kobayashi, M. Sugiura, H. Kitagawa, W. W.-L. Lam, *Chemical Reviews*, 2002, **102**, 2227.
- ³⁰ J.-F. Gal, C. Iacobucci, I. Monfardini, L. Massi, E. Duñach, S. Olivero, *Journal of Physical Organic Chemistry*, 2013, **26**, 2, 87-97.
- ³¹ Y. Yao, K. Nie, *Rare Earth Elements*, ed. D. A. Atwood, 2012, 459-474.
- ³² C. Le Roux and J. Dubac, *Synlett*, 2002, **2**, 181.
- ³³ W. Kern and V. Jaacks, *Journal of Polymer Science*, 1960, **48**, 399.
- ³⁴ M. Kučera and E. Spousta, *Makromolekulare Chemie*, 1965, **82**, 60.
- ³⁵ H. Baader, V. Jaacks and W. Kern, *Makromolekulare Chemie*, 1965, **82**, 213.
- ³⁶ H. D. Hermann, E. Fischer, K. Weissmermel, *Makromolekulare Chemie*, 1966, **90**, 1.
- ³⁷ V. Jaacks, H. Baader and W. Kern, *Makromolekulare Chemie*, 1965, **83**, 56.
- ³⁸ H. D. Hermann, *Makromolekulare Chemie*, 1966, **99**, 35.
- ³⁹ K. Weissmermel, E. Fischer, K. Gutweiler, H. D. Hermann and H. Cherdrón, *Angewandte Chemie International Edition*, 1967, **6**, 526.
- ⁴⁰ N. Brown, *Journal of Macromolecular Science: Part A*, 1967, **2**, 209.
- ⁴¹ O. Vogl, *Journal of Macromolecular Science: Part C*, 1975, **1**, 109.
- ⁴² F. Morelli, R. Tartarelli and G. Masetti, *European Polymer Journal*, 1968, **4**, 555.
- ⁴³ V. Jaacks, K. Boehlke and E. Eberius, *Die Makromolekulare Chemie*, 1968, **118**, 354.
- ⁴⁴ K. Brzezińska, W. Chwiałkowska, P. Kubisa, K. Matyjaszewski and S. Penczek, *Makromolekulare Chemistry*, 1977, **178**, 2491.
- ⁴⁵ D. Engel, *PEXACT 3.0.7-Software for Quantitative Spectroscopy and Chromatography*, S•PACT GmbH, Aachen, Germany, 2013.